$k\varepsilon\alpha$: a three-equation eddy-viscosity model of turbulence

Federico Ghirelli
Department of Energy and Environment, Chalmers University of Technology, Göteborg, Sweden

Abstract

Purpose – To provide an eddy-viscosity turbulence model that accounts for the non-equilibrium shape of the energy spectrum and for the effect of velocity correlation on turbulent viscosity.

Design/methodology/approach – The turbulence model is built using the standard $k\varepsilon$ model as the starting point. It is suggested that the character of turbulence depends on the time elapsed since its generation. Therefore, a local variable named "age of turbulence" or α, is defined and its transport equation is derived. Two hypotheses are formulated. The first one is that the shape of the energy spectrum depends on α. The second one is that also the effect of velocity correlation on turbulent viscosity is a function of α, in analogy with the dispersion coefficient of a particle in a turbulent flow. Hence, expressions for the characteristic time scale τ_T and the turbulent viscosity ν_T are proposed and they are integrated in the standard $k\varepsilon$ model, resulting in a three equation model named here $k\varepsilon\alpha$. The expressions of ν_T and τ_T reduce to those of the $k\varepsilon$ model in decaying turbulence, and deviate from them in recently produced turbulence. The empirical constants are calibrated and various benchmark experiments are simulated.

Findings – A comparison between computed results and experimental data show that the $k\varepsilon\alpha$ model is generally more accurate than the standard $k\varepsilon$ model.

Originality/value – The "age of turbulence" has not been used previously to characterise turbulence. The work is especially relevant for combustion/reacting applications, where the expression of the characteristic turbulence time scale is crucial for the estimation of the reactant mixing rates.

Keywords Turbulence, Shearing, Jets, Diffusion

Paper type Research paper

Nomenclature

C	= empirical constant
d	= nozzle diameter
D	= diffusivity
E	= power spectra
f	= empirical function
G	= production of k
H	= step height
k	= turbulent kinetic energy
ℓ	= length scale
m	= decay exponent
n	= integer constant
s	= auxiliary variable (time)
S	= strain rate tensor
Sc	= turbulent Schmidt number
t	= time
u, v, w	= velocities
U	= mean velocity
x	= coordinate
X	= mass fraction of a chemical species
Y	= distance from wall
Z	= generic transported scalar
α	= age of the turbulence (or of a scalar)
ε	= turbulence dissipation rate
λ	= auxiliary function
κ	= VonKarman constant
ν	= kinematic viscosity
ϕ	= generic variable
σ	= empirical constant
τ	= time scale
ω	= specific dissipation rate, frequency

Subscripts

0	= initial
A	= chemical species A
i	= integer index
j	= integer index
T	= turbulent

Further, explanation of the symbols is given in the text.

International Journal of Numerical Methods for Heat & Fluid Flow
Vol. 17 No. 2, 2007
pp. 140-164

0961-5539
DOI 10.1108/09615530710723939

Introduction

Linear two-equation models of turbulence are popular due to their robustness, and have been developed extensively. Since, it is known, however, that these models suffer certain shortcomings, a number of more advanced approaches have been developed, as for example nonlinear eddy-viscosity models, multi-scale models, Reynolds-stress models and large-eddy simulation (LES).

Two-equation models are based on the intrinsic assumption that two variables are sufficient to estimate the characteristic (integral) scales of turbulent motion. In fact, for given values of the two transported variables, typically k and ε characteristic time and length scales are derived from the theory of Kolmogorov. The hypotheses of Kolmogorov, however, are valid for small scale turbulent motion only (the inertial range), while the characteristic scales of turbulence lay in the energy containing range.

Multi-scale models of turbulence are based on the idea that the shape of the energy spectrum is decisive and that more than two variables can be used to describe it better. Such models can be found for example in Hanjalic *et al.* (1980), Kim and Chen (1989) and Rubinstein (2000).

Also nonlinear eddy-viscosity models and Reynolds-stress models are often more accurate than linear eddy-viscosity models. These models, however, are based on other considerations than multi-scale models, and usually they are not focussed on the shape the spectrum.

Alternatively, the large-scale motions can be computed by means of LES, but LES is computationally expensive. In fact, many of the calculations in the industrial sector are still performed by means of two-equation eddy-viscosity models.

In the present work, a transport equation is formulated and it is added to those of the standard $k\varepsilon$ model resulting in a new three-equation model of turbulence. The information from the additional equation is used to provide a more accurate estimation of the turbulent viscosity, based on considerations on the evolution of the spectrum, as it is done in multi-scale models. The additional equation in the present model, however, is completely different from those in multi-scale models, and does not require modelling of the source terms.

The $k\varepsilon$ model: expression of the turbulent viscosity

According to the cascade representation of turbulence, turbulent energy is produced at the large-scales (energy containing range), it is transported through the inertial sub-range, and it is dissipated in the dissipation range. The theory of Kolmogorov provides a universal description of the vortex structure in the inertial subrange in the form of relations between length, time and velocity scales:

$$u(\ell) \propto (\varepsilon \ell)^{1/3} \tag{1}$$

$$\tau(\ell) \propto \ell^{2/3} \varepsilon^{-(1/3)} \tag{2}$$

where ℓ are the length scales, u are the velocity scales, τ the time scales, and ε the turbulent energy dissipation rate. The validity of these relations is often extended to the larger scales of turbulence, as, for example, in the $k\varepsilon$models. An important question is then: to what extent are these relations valid outside the inertial subrange?

In the $k\varepsilon$ model of Launder and Spalding (1974), also known as standard $k\varepsilon$ the expression for the turbulent viscosity is based on the analogy with the expression for molecular viscosity according to kinetic theory of gases:

$$\nu \propto \ell_{\text{free path}} u_{\text{molecular}} \tag{3}$$

where ν is the molecular viscosity, $\ell_{\text{free path}}$ the mean free path of a molecule, and $u_{\text{molecular}}$ the molecular velocity due to temperature.

By analogy the turbulent viscosity can be written:

$$\nu_{\text{T}} \propto \ell_{\text{T}} u_{\text{T}} \tag{4}$$

where the subscript T refers to characteristic turbulent quantities. This analogy was first used by Prandtl to formulate the mixing length hypothesis. The physical meaning of the characteristic length scale of turbulence ℓ_{T} has not been defined rigorously (Pope, 2000), but it is reasonable to expect that ℓ_{T} should be comparable to the integral length scales. The same can be said about characteristic time scale τ_{T}. The characteristic velocity scale of turbulence u_{T} is:

$$u_{\text{T}} = \left\langle u'^2 + v'^2 + w'^2 \right\rangle^{1/2} = (2k)^{1/2} \tag{5}$$

where u' v' and w' are the fluctuating components of velocity in the Reynolds (or Favre) averaging, and k is the turbulent kinetic energy.

In the $k\varepsilon$model, transport equations are solved for the two variables k and ε which are used to characterise the turbulence. The turbulent viscosity is then computed by substituting equations (1) and (5) into equation (4):

$$\nu_{\text{T}} \propto k^2/\varepsilon \tag{6}$$

The $k\varepsilon$model: relations between the turbulent variables

The relations between the turbulent variables k, ε τ_{T}, ℓ_{T}, ν_{T} for given k and ε are fixed when three independent relations are defined. In the k-εmodel the three relations are equations (1), (2) and (4). Some of the resulting relations are summarized in Table I.

The question about the validity of equations (1) and (2) outside the inertial subrange, then, could be reformulated as follows: are two variables sufficient to characterize the turbulence? Could the model be improved by introducing new independent variables?

First hypothesis: considerations about the spectrum

In experiments where turbulence is generated by means of a grid, the larger generation of turbulence takes place in the zone directly following the grid. Near the grid,

		ν_T		ε		τ_T		ℓ_{T}
ν_T	=			$c_\mu k^2 \varepsilon^{-1}$	$\propto$	$\tau_{\text{T}} k$	$\propto$	$\ell_{\text{T}} k^{-(1/2)}$
ε	=	$c_\mu k^2 \nu_T^{-1}$		$\propto$		$k\tau^{-1}$	$\propto$	$k^{3/2} \ell_T^{-1}$
τ_T	$\propto$	$k^{-1} \nu_{\text{T}}$	$\propto$	$k\varepsilon^{-1}$		$\propto$		$\ell_{\text{T}} k^{-(1/2)}$
ℓ_{T}	$\propto$	$k^{-(1/2)} \nu_{\text{T}}$	$\propto$	$k^{3/2} \varepsilon^{-1}$	$\propto$	$\tau_{\text{T}} k^{1/2}$		

Table I.
Relations between the turbulent variables in the $k\varepsilon$ model

turbulence is strongly anisotropic and non-homogeneous, while at larger distances, where it decays, turbulence is more homogeneous and isotropic. It seems therefore that the whole turbulent motion, after its generation, develops towards a homogeneous and isotropic state (which resembles the inertial subrange described by Kolmogorov in his hypotheses). At the early stage of turbulence, i.e. near the grid, one would therefore expect that the inertial range is relatively narrow, and that it becomes larger as turbulence develops, including a broader part of the energy spectrum. At the early stage of turbulence, furthermore, the relations between the characteristic scales should deviate more significantly from equations (1) and (2), which are derived from the hypotheses of homogeneity and isotropicity. According to this analysis, the wake behind the grid could be imagined to shift from an early stage to a late stage:

- in the early stage dissipation is smaller than generation and turbulence is highly anisotropic and non-homogeneous, and it is characterised by a relatively narrow inertial subrange; and
- in the late stage dissipation is larger than generation and turbulence is almost isotropic and homogeneous, and the inertial subrange is broader.

One could then say that turbulence undergoes an ageing process, where "old" turbulence is characterized by a broader inertial subrange than "fresh" turbulence.

Going back to the question whether k andε are sufficient to characterize the turbulence, it could be reformulated as follows: could two different turbulent spectra share the same turbulent energy and dissipation rate? In Figure 1, two hypothetical energy spectra are shown that have the same k andε but different integral time scale (the same reasoning can be repeated for the length scales).

Consistent with the argument on ageing of turbulence, spectrum $E_1(\omega)$ could characterise an "older" turbulence than that of spectrum $E_2(\omega)$. The "age" of the turbulence could then be a useful parameter for characterizing the scales.

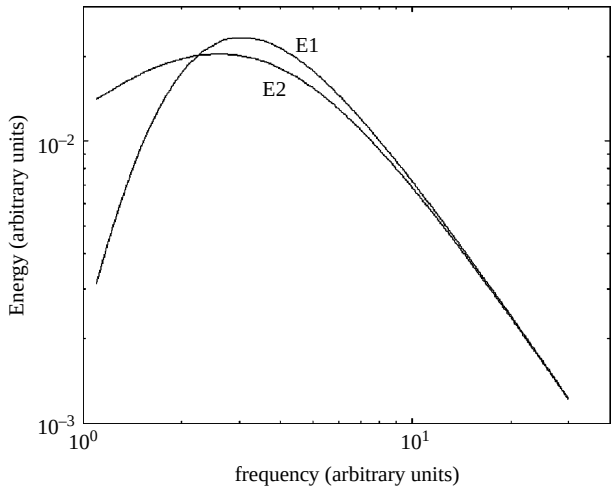

Figure 1.
Two different energy spectra characterised by the same values of k and ε

The α-equation

Ghirelli and Leckner (2004) showed how the residence time of a reacting species in a flow can be computed by means of transport equations. In a constant-density turbulent flow where molecular diffusion is negligible compared to turbulent diffusion, the transport equation for a chemically reacting species A can be written:

$$\frac{DX_A}{Dt} = \frac{\partial}{\partial x_i}\left(D_{\mathrm{T}}\frac{\partial X_A}{\partial x_i}\right) + s_P - s_C \tag{7}$$

where X_{A} is the mass fraction of the species, D_{T} is the turbulent diffusivity, s_{p} is the source term due to reactions that produce A and s_{c} is the sink term due to reactions that consume A.

The local residence time (or age) of A can be computed by means of a transport equation, which is written (Ghirelli and Leckner, 2004):

$$\frac{D(X_A\alpha_A)}{D_t} = \frac{\partial}{\partial x_i}\left(D_{\mathrm{T}}\frac{\partial(X_A\alpha_A)}{\partial x_i}\right) + X_A - \alpha_A s_C \tag{8}$$

where α_{A} is the age of A.

The turbulent energy k, as the mass fraction of a species in a reacting flow, is a scalar which is produced, transported and consumed within the flow. This mathematical similarity is clear if equation (7) is compared with the transport equation of k that is used in several models, including the standard $k\varepsilon$:

$$\frac{Dk}{Dt} = \frac{\partial}{\partial x_i}\left(D_k\frac{\partial k}{\partial x_i}\right) + G - \varepsilon \tag{9}$$

In this equation, D_{k} is the effective diffusivity of k, G is its production term andε its dissipation. Starting from equation (9) and repeating the derivation of equation (8), it is possible to obtain an analogous transport equation for the local residence time of the turbulent energy α_{k} (or, more briefly, age of the turbulence α). The equation is written, in a constant density flow:

$$\frac{D(k\alpha)}{Dt} = \frac{\partial}{\partial x_i}\left(D_k\frac{\partial(k\alpha)}{\partial x_i}\right) + k - \alpha\varepsilon \tag{10}$$

The derivation of equations (8) and (10) is presented in the Appendix.

Second hypothesis: dispersion analogy

The turbulent dispersion of a fluid particle injected from a point source into a homogeneously turbulent flow can be modelled by a turbulent diffusivity D_{T} that depends on the time t elapsed since the injection of the particle as follows (Pope, 2000):

$$D_{\mathrm{T}}(t) = \overline{u'^2}\int_0^t \rho(s)\mathrm{d}s \tag{11}$$

where $\rho(s)$ is the Lagrangian velocity autocorrelation function, which, according to the Langevin model and to experimental data (Pope, 2000), can be expressed as:

$$\rho(s) \equiv \frac{\langle u(t)u(t+s)\rangle}{\langle u^2(t)\rangle} = \exp\left(-\frac{s}{\tau_T}\right) \tag{12}$$

Substituting equations (5) and (12) in (11) one gets:

$$D_T(t) = \frac{2}{3}k\tau_T\left(1 - \exp\left(-\frac{t}{\tau_T}\right)\right) \tag{13}$$

Equation (13) shows that the dispersion of a fluid particle in a turbulent flow can be modelled by means of a diffusivity that is nearly constant for large relative residence times t/τ_T, and that is nearly proportional to t for small t/τ_T. Turbulent diffusion as expressed by equation (13) is smaller at short residence times than at large residence times because the turbulent velocities are correlated within small time intervals. After a sufficiently large residence time, the correlation is sufficiently small to be neglected. The exponential term in equation (13) is therefore referred to as the "effect of correlation".

It is reasonable to assume that the loss of correlation of the turbulent velocity (energy) with its age is analogous to the loss of correlation of the velocity of a Lagrangian particle with time.

On the basis of the above assumption, considering that $D_T = \nu_T/Sc_T$ (Sc_T is the turbulent Schmidt number) the expression for the turbulent viscosity is written:

$$\nu_T = \frac{2}{3}Sc_T k\tau_T\left(1 - \exp\left(-c_\alpha\frac{\alpha}{\tau_T}\right)\right) \tag{14}$$

where c_α is a corrective constant. If the relation $k \propto \ell^2/\tau_T^2$ (from in Table I) is still taken to be valid, then the expression of ν_T in equation (14) tends to the expression in equation (4) for large relative ages α/τ_T. The expression for the turbulent viscosity in equation (4) could be therefore dropped in favour of the one in equation (14), which accounts for the correlation of turbulent velocities.

The exponential term in equation (14) is named the "model effect of correlation" or γ:

$$\gamma \equiv \exp\left(-c_\alpha\frac{\alpha}{\tau_T}\right) \tag{15}$$

Clearly, γ varies between 0 and 1 and it decreases as α/τ_T grows. The constant c_α is introduced in equation (14) for the reason explained in the following.

Turbulence at a point in the domain is a superposition of fluctuations that have been generated at various locations upstream of the point. Therefore, the turbulence at a point has been produced during an interval of time rather than at one discrete time. In fact, the value computed by equation (10) is an energy-weighted average of the age of turbulence, as it is seen in the Appendix. Let us consider, for example, the distribution of a generic variable on the frequency domain $\phi(\omega)$. Its energy average is defined as:

$$\langle\phi\rangle = \frac{1}{k}\int_0^\infty E(\omega)\phi(\omega)d\omega. \tag{16}$$

The age of turbulence as a function of the frequency $\alpha(\omega)$ should be an increasing function of ω because in the energy cascade the energy flows from the large-scales to

the small ones. Even though $\alpha(\omega)$ is not known, it is clear that the average effect of the correlation and the effect of correlation of the average age $<\alpha>$ differ:

$$\left\langle \exp\left(-\frac{\alpha(\omega)}{\tau_T}\right)\right\rangle \neq \exp\left(-\frac{\langle\alpha(\omega)\rangle}{\tau_T}\right) \tag{17}$$

In fact the left hand side of equation (17) is generally larger than its right hand side. In the expression of the turbulent viscosity, it is the average effect of correlation that should be accounted for, rather than the right hand side of equation (17), but there is not enough information to compute the left hand side (neither $\alpha(\omega)$ or $E(\omega)$ are known), and therefore it is approximated according to equation (15), that is, with a model effect of correlation. The empirical constant c_α is calibrated to give good agreement with experimental results.

Characteristic scale function

According to the reasoning about the ageing of turbulence, for a given k and a given ε the characteristic scales τ_T and ℓ_T should decrease with α (Figure 1). Additionally, according to the cascade representation of turbulence, energy is mainly transferred from larger to smaller scales. This also seems to support the hypothesis that for given values of k and ε the scales should decrease with α (or with the relative age α/τ_T). It is therefore reasonable to assume that, in analogy with the relation $\tau_T \propto k/\varepsilon$ in Table I, the characteristic time scale in the $k\varepsilon\alpha$ model can be written as:

$$\tau_T = c_\tau \frac{k}{\varepsilon} f\left(\frac{\alpha}{\tau_T}\right) \tag{18}$$

where f is a decreasing function of α/τ_T and c_τ is an empirical constant. Not much else is known about the function f; its expression is therefore determined by trial and error in the following simulations of benchmark flows. The following expression for f has given the best results:

$$f = \frac{1-\gamma^n}{1-\gamma} = \sum\nolimits_{i=0}^{n-1} \gamma^i \tag{19}$$

Introducing equations (18) and (19) into equation (15), it follows that:

$$\gamma = \exp\left(-\frac{c_\alpha \alpha \varepsilon}{c_\tau k \sum_{i=0}^{n-1} \gamma^i}\right) \tag{20}$$

For a given set of k, ε and α solving numerically equation (20) gives γ.

The $k\varepsilon\alpha$ model: relations between the turbulent variables

As for the $k\varepsilon\alpha$ model, in the $k\varepsilon\alpha$ model the relations between the turbulent variables k, ε, α, τ_T, ℓ_T, ν_T for given k, ε and α are fixed when three independent relations are defined. The first and second relations are equations (14) and (18). The third relation is taken to be $k \propto \ell_T^2/\tau_T^2$, which is the last expression in the last row of Table I. Some resulting relations between the turbulent variables in the $k\varepsilon\alpha$ model are reported in Table II.

	ν_T		ε		τ_T		ℓ_T
ν_T		$=$	$(2/3)Sc_T c_\tau k^2 \varepsilon^{-1}(1-\gamma'')$	$=$	$(2/3)Sc_T \tau_T k(1-\gamma)$	$\propto$	$\ell_T k^{-(1/2)}(1-\gamma)$
ε	$=$	$(2/3)Sc_T c_\tau k^2 \nu_T^{-1}(1-\gamma'')$	$=$	$c_\tau k \varepsilon^{-1} f$	$\propto$	$k^{3/2}\ell_T^{-1} f$
τ_T	$=$	$(3/2)Sc_T k^{-1}\nu_T(1-\gamma)^{-1}$	$=$	$c_\tau k \varepsilon^{-1} f$	$\propto$	$\ell_T k^{-(1/2)}$
ℓ_T	$\propto$	$k^{-(1/2)}\nu_T(1-\gamma)^{-1}$	$\propto$	$k^{3/2}\varepsilon^{-1} f$	$\propto$	$\tau_T k^{1/2}$

Table II.
Relations between the turbulent variables in the $k\varepsilon\alpha$ model

A comparison between Tables I and II reveals that Table II includes more equalities. This is due to the fact that equations (11)-(13) are not only a result of dimensional reasoning, but they result from stochastic modelling and are verified experimentally (Pope, 2000).

It was mentioned that the expression of the turbulent viscosity $\nu_T = 2/3(Sc_T c_\tau k^2 \varepsilon^{-1}(1 - \gamma^n))$ tends to equation (6) for large α/τ_T. It is also interesting to notice that the expression tends to equation (6) also for large values of n. In the examined flows, the factor $(1 - \gamma^n)$ deviates significantly from unity it the regions characterised by high velocity gradients.

The $k\varepsilon\alpha$ model

The $k\varepsilon\alpha$ model is a development of the $k\varepsilon$ model. The introduction of the α-equation and the new expression of the turbulent viscosity are the structural changes performed on the original model. The transport equations of k and ε are rewritten with minor changes from the standard version of the two-equation model (Launder and Spalding, 1974). The $k\varepsilon\alpha$ model can be summarized in terms of equations as follows:

$$\frac{Dk}{Dt} = \frac{\partial}{\partial x_i}\left(\left(\nu + \frac{\nu_T}{\sigma_k}\right)\frac{\partial k}{\partial x_i}\right) + G - \varepsilon \tag{21}$$

$$\frac{D\varepsilon}{Dt} = \frac{\partial}{\partial x_i}\left(\left(\nu + \frac{\nu_T}{\sigma_\varepsilon}\right)\frac{\partial \varepsilon}{\partial x_i}\right) + c_1\frac{\varepsilon}{k}G - c_2\frac{\varepsilon^2}{k} \tag{22}$$

$$\frac{D(k\alpha)}{Dt} = \frac{\partial}{\partial x_i}\left(\left(\nu + \frac{\nu_T}{\sigma_k}\right)\frac{\partial (k\alpha)}{\partial x_i}\right) + k - \alpha\varepsilon \tag{23}$$

$$\nu_T = \frac{2}{3}Sc_T c_\tau \frac{k^2}{\varepsilon}(1 - \gamma^n) \tag{24}$$

$$\gamma = \left(\exp - \frac{c_\alpha \alpha \varepsilon}{c_\tau k \sum_{i=0}^{n-1}\gamma^i}\right) \tag{25}$$

where G is the production term, which is a function of the rate of strain tensor S_{ij}:

$$G = 2(\nu + \nu_T)S_{ij}S_{ij} \tag{26}$$

The minor change introduced in the equations from the $k\varepsilon$model is the addition of the molecular viscosity to the turbulent viscosity. The molecular viscosity is generally negligible in turbulent flows, but it can stabilize somewhat the numerical solution in areas where the values of k andε approach zero, often present in the computational domain. This change is merely a measure to improve numerical behaviour and does not mean that the model is intended for low-Reynolds-number flows.

Model constants

The $k\varepsilon\alpha$ model includes seven empirical constants: c_τ, c_α, c_1, c_2, σ_k, σ_ε and n. The constants σ_k, σ_ε, c_α and n are chosen to give good agreement with the following benchmark flows. The best set of constants found is:

$$\sigma_k = 0.6\ \sigma_\varepsilon = 1 n = 16\ c_\alpha = 0.2 \tag{27}$$

To estimate the model constants c_τ, c_1 and c_2, experimental data from decaying grid turbulence and boundary layers. In the logarithmic-law region of the boundary layer, the following relations hold:

$$\varepsilon = G = \frac{u_\tau^3}{\kappa y} \tag{28}$$

$$k = \frac{u_\tau^2}{0.3} \tag{29}$$

$$\frac{\partial \bar{U}}{\partial y} = \frac{u_\tau}{\kappa y} \tag{30}$$

where $\kappa = 0.41$ is the Von Karman constant, u_τ is the friction velocity and y is the distance from the wall. From equations (24), (26), (28)-(30) therefore:

$$\begin{aligned} \varepsilon = G = \nu_T \left(\frac{\partial \bar{U}}{\partial y}\right)^2 = \frac{2}{3} Sc_T c_\tau \frac{k^2(1-\gamma^n)}{\varepsilon} \frac{u_\tau^2}{\kappa^2 y^2} \\ \Rightarrow \frac{2}{3} Sc_T c_\tau (1-\gamma^n) = \frac{\kappa^2 y^2 \varepsilon^2}{u_\tau^2 k^2} = \frac{\kappa^2 y^2}{u_\tau^2} \frac{0.3^2}{u_\tau^4} \frac{u_\tau^6}{\kappa^2 y^2} \Rightarrow \frac{2}{3} Sc_T c_\tau (1-\gamma^n) = 0.09 \end{aligned} \tag{31}$$

which implies that γ^n is constant and α/τ_T is either constant or sufficiently large (for example, $\alpha/\tau_\tau > 1.5 => \gamma^n < 0.01$) in the log-law region. If α/τ_τ is large, taking $Sc_T = 0.7$ gives $c_\tau \approx 0.19$. If α/τ_τ is constant then:

$$\alpha = c_4 \tau_T = c_4 c_\tau k f / \varepsilon \tag{32}$$

Equation (23) in the log-law region of the boundary layer can be written:

$$0 = \frac{\partial}{\partial y}\left(\frac{\nu_T}{\sigma_k} \frac{\partial (k\alpha)}{\partial y}\right) + k - \alpha\varepsilon \tag{33}$$

Because the rate of change in the direction of the flow is negligible. Substituting equations (15), (24), (28), (29), (31) and (32) into equation (33) gives:

$$c_4 = 7.4 Sc_T \left[1 - \exp(-c_\alpha c_4)\right] \left[\frac{1-\kappa^2}{(0.3\sigma_k)}\right]^{-1} \Rightarrow c_4 = \alpha/\tau_T \approx 78 \tag{34}$$

which is a large value of α/τ_T. It follows that α/τ_T is large (>1.5) in the log-law region of the boundary layer and $c_\tau = 0.19$.

In decaying homogeneous turbulence equations (21) and (22) can be written:

$$\frac{dk}{dt} = -\varepsilon \tag{35}$$

$$\frac{d\varepsilon}{dt} = -c_2 \frac{\varepsilon^2}{k} \tag{36}$$

and have solution (Pope, 2000):

$$k(t) = k_0\left(\frac{t}{t_0}\right)^{-m}, \quad \varepsilon(t) = \varepsilon_0\left(\frac{t}{t_0}\right)^{-(m+1)}, \quad t_0 = m\frac{k_0}{\varepsilon_0}, \quad m = \frac{1}{c_2 - 1} \tag{37}$$

The experimental value of the decay exponent m is 1.30 (Mohamed and LaRue, 1990), which corresponds to $c_2 = 1.77$.

Equation (22) in the log-law region of the boundary layer can be written:

$$0 = \frac{\partial}{\partial y}\left(\frac{\nu_T}{\sigma_\varepsilon}\frac{\partial \varepsilon}{\partial y}\right) + (c_1 - c_2)\frac{\varepsilon^2}{k} \tag{38}$$

(Because the rate of change in the direction of the flow is negligible and $\varepsilon = G$). Substituting equations (24), (28), (29), (31) into equation (38) gives:

$$c_1 = c_2 - \frac{\kappa^2}{0.3\sigma_\varepsilon} = 1.21 \tag{39}$$

Benchmark flows simulation

Five different flows are simulated with the standard $k\varepsilon$(Launder and Spalding, 1974) and the $k\varepsilon\alpha$ models. In order to assess the influence of the empirical constants on the performance of the models, the flows are also simulated with a modified $k\varepsilon$ model, where the constants c_1, c_2, σ_k and σ_ε have been substituted with the corresponding values from the $k\varepsilon\alpha$ model.

The first three flows are simulated by means of the commercial finite-volume solver Fluent 6.1.18. The software includes a default implementation of the standard $k\varepsilon$ model, but its source code is not available to the user. Therefore, in order to avoid any differences in the numerical implementation of the $k\varepsilon$ and $k\varepsilon\alpha$ model, both models are written as user-defined functions. A comparison between the default $k\varepsilon$ and the user-defined $k\varepsilon$ shows negligible differences. The SIMPLE pressure-velocity coupling algorithm and second order accurate discretization are applied. The fourth and fifth flows are modelled by means of simplified transport equations. The simulation is therefore performed with a different solver, further specified in Section 11.4.

Flow over a backward-facing step

The computational domain for the simulation of the experiment of Adams and Eaton (1988) is shown in Figure 2.

The grid is made of square cells of side 2 mm (the height of the step is $H = 38$ mm). Adams and Eaton (1988) provide the mean velocity profile at the inlet and specify that the upstream flow behaves like a flat-plate boundary layer. Therefore, the boundary conditions at the inlet are given to resemble a flat-plate boundary layer. The age of the turbulence is taken to be $\alpha = 2\tau_T$, in consideration of the reasoning on the log-law region made in Section 10. Turbulence at the wall-adjacent cells is given by a wall

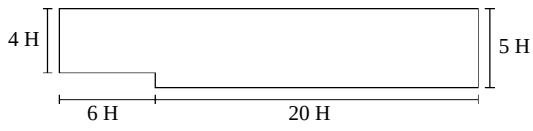

Figure 2.
Computational domain for the experiment of Adams and Eaton (1988)

function suggested by Jones (1994); production and dissipation rates are assumed to be equal and given by:

$$G = \varepsilon = \frac{(0.3k)^{3/2}}{\kappa y} \tag{40}$$

where y is the distance between the cell centre and the wall. The ε-equation is not solved at the wall-adjacent cells; instead the value of ε is given by equation The k-equation is solved at the wall-adjacent cells and a zero-gradient boundary condition is specified at the walls. The effective viscosity at the centre of the wall-adjacent cells is given by:

$$\nu_{eff} = \nu + \nu_{\mathrm{T}} = \frac{\kappa(0.3k)^{1/2}}{\ln(9.8y^*)}\, y \tag{41}$$

where y^* is a scaled distance from the wall:

$$y^* = \frac{(0.3k)^{1/2}}{\nu}\, y \tag{42}$$

The α-equation is unchanged at the wall adjacent cells, and a zero-gradient boundary condition is given at the walls. In most of the wall-adjacent cells $35 < y^* < 60$, except for the reattachment zone, where y^* reaches a maximum value of 100, and at the concave corner of the step, where y^* reaches a minimum value of 7. Around the reattachment point and the concave corner, the wall function is not expected to be accurate, since it is built on data from developed boundary layers. In these locations, however, the velocities and the strain rates are relatively small, so that the inaccuracy of the wall function should not affect significantly the outer flow field.

The dependence of the solution to the grid is checked by simulating the flow on a grid of square cells with a side of 1 mm, except for the cells adjacent to the walls, which have 2 mm sides in order to keep the centre of the cell in the log-law layer (the grid is unstructured). The solutions from the two grids present negligible differences. The experimental and computed mean velocity fields are compared in Figures 3(a) and (b).

The standard $k\varepsilon$and the $k\varepsilon\alpha$ models predict very similar results (the two curves almost coincide), which agree very well with the measured velocities, except in the vicinity of the reattachment point. The modified $k\varepsilon$ model is significantly less accurate.

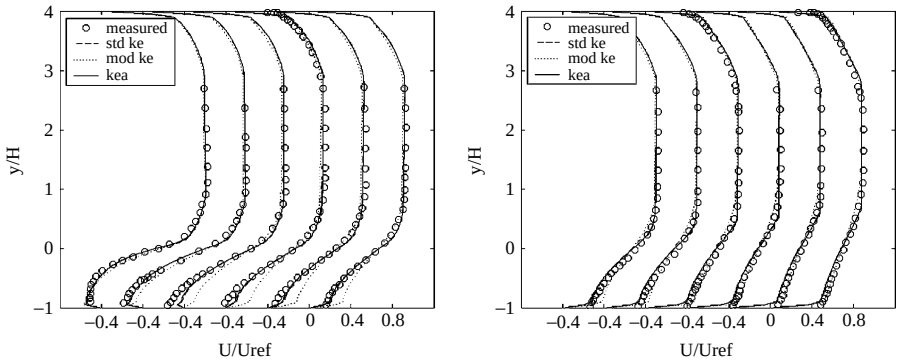

Figure 3.
(a) and (b) Computed and measured mean velocities at various sections downstream from the step

Notes: Sections position (left to right): x/H= 2.0, 3.33, 4.67, 6.0, 6.67, 7.33, 8.67, 10.0, 12.0, 14.0, 16.0, 18.0

The distance between the step and the reattachment point is underpredicted by all models as shown in Table III.

The discrepancy around the reattachment point might be due to the mentioned inaccuracy of the wall function in this area. Considering this and the very good agreement obtained in the remaining part of the domain, it might be argued whether the position of the reattachment point is a significant indicator of the quality of the turbulence model or of the wall function.

Axisymmetric jet

A schematic picture of the domain for the simulation of the axisymmetric, momentum-conserving jet measured by Hussein *et al.* (1994) is shown in Figure 4.

The room surrounding the jet and the equipment has a square section and therefore is not axisymmetrical. However, the distance of the room walls from the measured part of the jet is so large that the room can be modelled as cylindrical with good approximation. The radius of the cylinder is such that the cross section of the modelled room is equal to that of the actual room. The computational grid in this case is unstructured, with higher node density in the vicinity of the nozzle. The number of cells employed is about 190,000 and grid independence was checked by further increasing grid density by a factor 4 (dividing each cell in four). The size of the cells adjacent to the room wall is suitable for the application of the wall function, but the size of the cells adjacent to the nozzle wall is too small for the wall function to be applied. Detailed models of turbulence next to walls are available, which can describe turbulence in the viscous wall region. One such model, denominated "enhanced wall treatment" is implemented in the software used (Fluent Inc., 2003). The use of the default enhanced wall treatment is simple, but the implementation of such model by the user is overly laborious, especially in consideration of the fact that the flow in question is a typical free shear flow, i.e. a flow where the influence of the walls is unimportant. Therefore, rather than implementing the enhanced wall treatment in the user-defined turbulence models, a comparison was made to assess whether a simplified approach could be used. The comparison is between two simulations of the flow performed with the standard $k\varepsilon\alpha$ in the first one, the default implementation of the enhanced wall treatment is used, in the second one a simplified treatment of turbulence

Meas.	SD $k\varepsilon$	$k\varepsilon\alpha$	Mod. $k\varepsilon$
6.6	5	5	4.3

Table III.

Note: Measured and computed distances between the step and the reattachment point

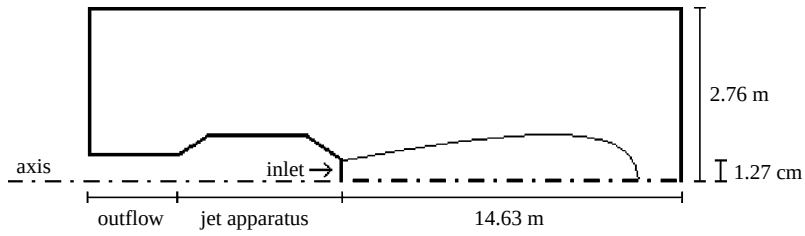

Figure 4.
Computational domain (not in scale)

is applied at the nozzle-wall-adjacent cells. The simplified treatment consists of using a zero-gradient boundary condition for k and ε and setting the effective viscosity equal to the molecular viscosity at the nozzle-wall-adjacent cells. The comparison shows that the choice of the wall treatment have no detectable effect on the measured part (and the main body) of the jet, and therefore the simplified treatment is used at the nozzle-wall-adjacent cells in all the simulations discussed in the following.

For the inlet boundary condition, the value of k is given by Hussein *et al.* (1994). The relative age and the characteristic length scale of the turbulence are assumed to be $\alpha/\tau_T = 2$ and ℓ or $\ell_T = 0.07d$, where d is the diameter of the nozzle. The relative age at the inlet is set according to what is considered to be a reasonable value, since no experimental data are available about this variable. Therefore, the sensitivity of the solution to the inlet value of the relative age is analysed in the interval $0.5 \leq \alpha/\tau_T \leq 5$ and it is found to be negligible. The insensitivity of the solution to this boundary condition is expected because turbulent energy is mainly produced inside the simulation domain. The flow of the third scalar ($k\alpha$) from the inlet is therefore small compared to its generation inside the domain. From a simulation setup point of view, the insensitivity is desirable, because it implies that the value of α at the inlet does not need to be specified accurately.

The measured and computed axial velocities are compared in Figures 5 and 6. The measured and computed spreading rates in the interval $30 < x/d < 120$ are reported in Table IV.

The measured and computed turbulence intensities are shown in Figure 7. The integral length scales were not measured by Hussein *et al.* (1994), but Wygnanski and Fielder (1969) did so in an analogous axisymmetric jet. By considering non-dimensional variables is therefore possible to compare the scales computed for the jet of Hussein *et al.* (1994) with the ones measured by Wygnanski and Fielder (1969). Since, the relation defining the length scale in the models is only a proportionality relation, a comparison can only be made in terms of relative scales. This is done in Figure 8.

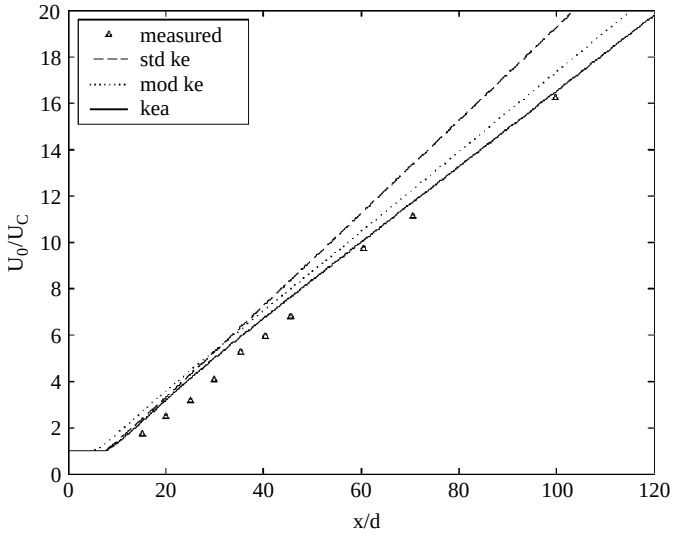

Figure 5.
Mean axial velocities along the axis of the jet

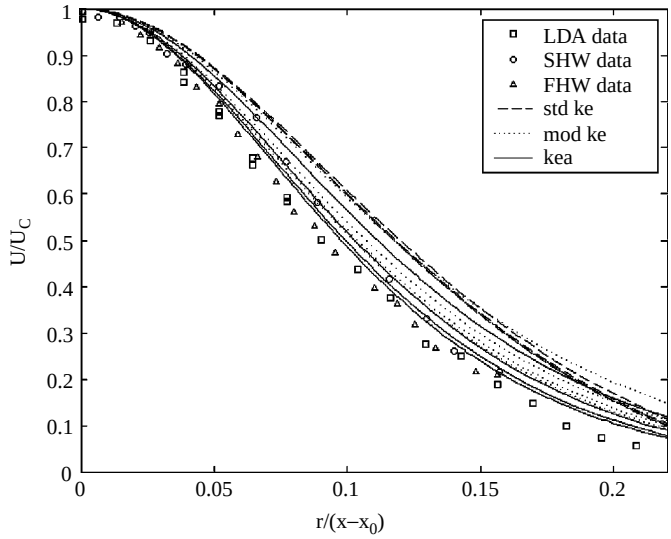

Figure 6.
Mean axial velocities at sections $x/d = 30, 60, 90, 120$

Table V.
Measured and computed spreading rates in the planar jet flow

Meas.	SD $k\varepsilon$	$k\varepsilon\alpha$	Mod. $k\varepsilon$
0.094	0.118	0.095	0.098

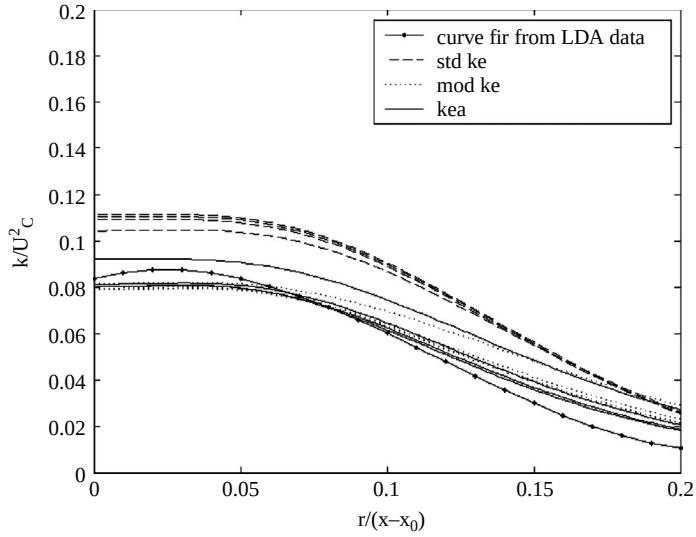

Figure 7.
Turbulence intensities at sections $x/d = 60, 90, 120$

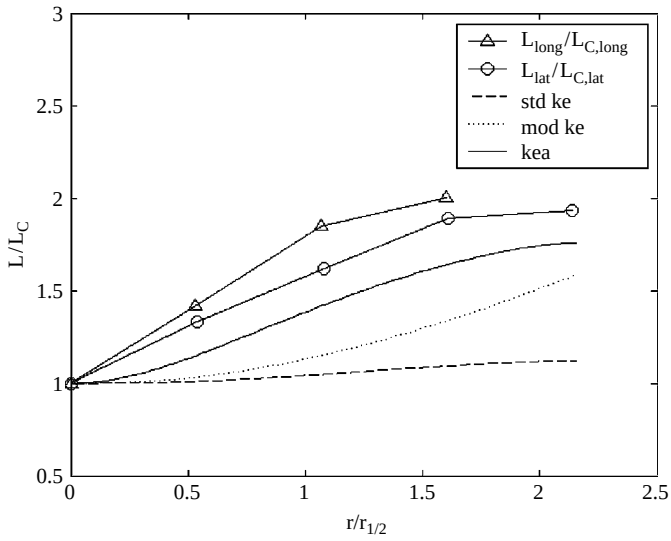

Figure 8.
Length scales at section $x/d = 90$

All the figures and the table show that the results of the $k\varepsilon\alpha$ model are in better agreement with the experimental data than those of the standard $k\varepsilon$model. Figure 6 shows that the $k\varepsilon\alpha$ model predicts a slower approach to self-similarity than the standard $k\varepsilon$ model does. The results of the modified $k\varepsilon$ model lay in between those of the standard $k\varepsilon$ and the $k\varepsilon\alpha$ models.

Planar jet

The planar turbulent jet investigated by Gutmark and Wygnanski (1976) is simulated. The computational grid used is unstructured, with higher node density in the vicinity of the nozzle. The number of cells employed is about 130,000 and grid independence was checked by further increasing grid density by a factor 4. The computational domain is two-dimensional and plane-symmetrical across the jet.

Since, this is a free shear flow, the same simplified wall treatment is applied as in the axisymmetric jet case. The same check is also made to verify that the wall treatment does not affect the solution in the measured part of the jet.

For the inlet boundary condition, the value of k is given by Gutmark and Wygnanski (1976). The relative age and the characteristic length scale of the turbulence are assumed to be $\alpha/\tau_T = 2$ and ℓ *or* $\ell_T = 0.07d$, where d is the diameter of the nozzle. Also in this case the relative age at the inlet is set according to what is considered to be a reasonable value and the sensitivity of the solution to this boundary condition is found to be negligible in the interval $0.5 \leq \alpha/\tau_T \leq 5$.

Comparisons between measurements and computations are shown in Figures 9-13. The measured and computed spreading rates in the interval $65 < x/d < 118$ are reported in Table V.

In Figure 9, the modified $k\varepsilon$ model gives a better prediction than the standard $k\varepsilon$ and the $k\varepsilon\alpha$ models predictions, which are equivalent. In Figures 10 and 11 the predictions of the $k\varepsilon\alpha$ and the modified $k\varepsilon$ models are slightly superior to those of the standard $k\varepsilon$ model. In Figure 12 the $k\varepsilon$ model performs somewhat better than the

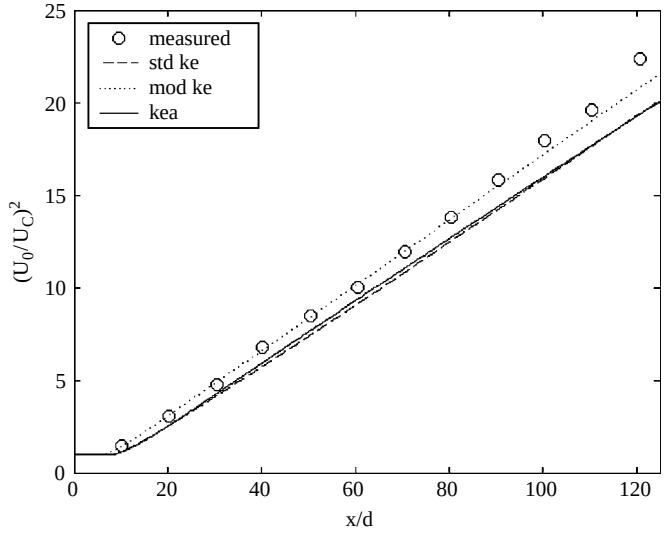

Figure 9.
Mean x-velocities on the symmetry plane

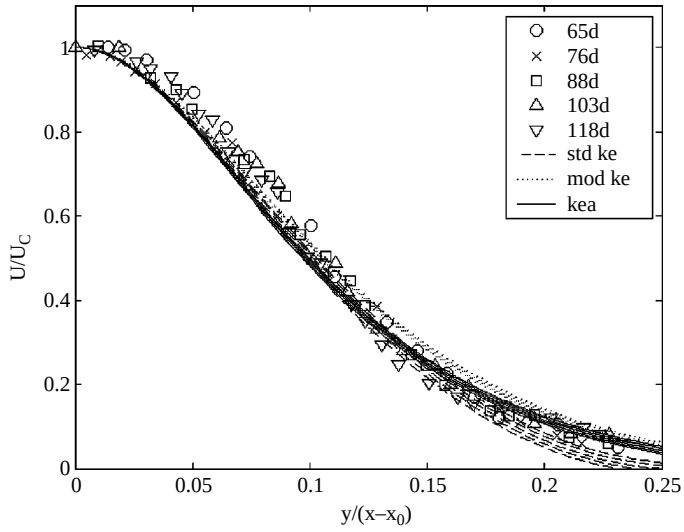

Figure 10.
Mean x-velocities across the jet, at sections $x/d = 65, 76, 88, 103, 118$

$k\varepsilon\alpha$ and the modified $k\varepsilon$ models and in Figure 13 the models are equivalent. Within the measurement accuracy, the spread rate is equally well predicted by the models.

It is interesting to notice that in this jet the $k\varepsilon\alpha$ model approaches self-similarity faster than the $k\varepsilon$model. Gutmark and Wygnanski (1976) state that: "The approach to self-preservation in a two-dimensional jet ... occurs much earlier than in an axisymmetric jet ..." (earlier in terms of x/d). Figures 6, 7, 10 and 12 show that $k\varepsilon\alpha$ model predicts this trend while the $k\varepsilon$ calculates the opposite behaviour.

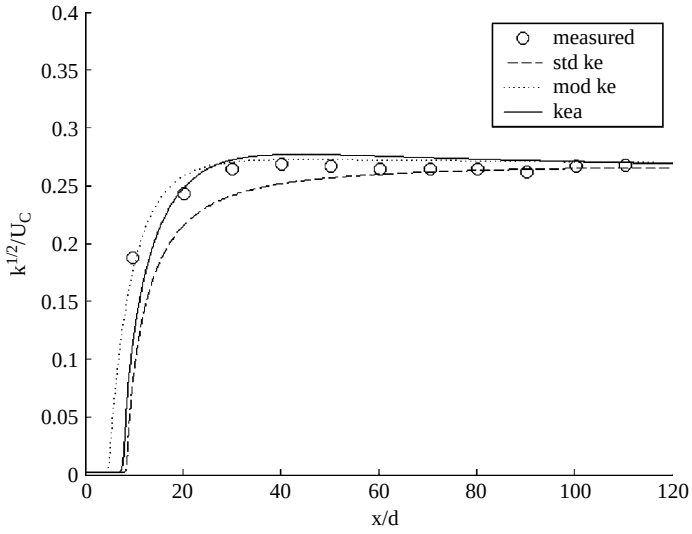

Figure 11.
Turbulence intensities on the symmetry plane

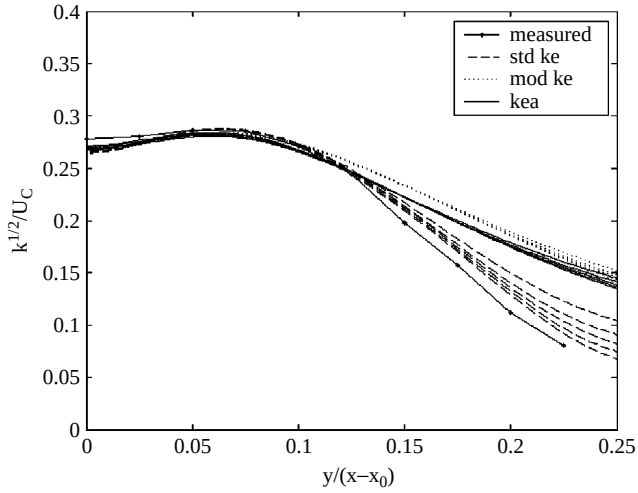

Figure 12.
Turbulence intensities across the jet, at sections $x/d = 95$, 106, 118, 129, 143

Nearly, homogeneous turbulent shear flow

In a nearly homogeneous shear flow, such as the ones described by Tavoularis and Corrsin (1981) and by Tavoularis and Karnik (1981) equations (21)-(25) can be approximated as:

$$U_1 \frac{\partial k}{\partial x_1} = c_\mu \frac{k^2}{\varepsilon}(1 - \gamma^n)\left(\frac{\partial U_1}{\partial x_2}\right)^2 - \varepsilon \tag{43}$$

$$U_1 \frac{\partial \varepsilon}{\partial x_1} = c_1 \frac{\varepsilon}{k} c_\mu \frac{k^2}{\varepsilon}(1 - \gamma^n)\left(\frac{\partial U_1}{\partial x_2}\right)^2 - c_2 \frac{\varepsilon^2}{k} \tag{44}$$

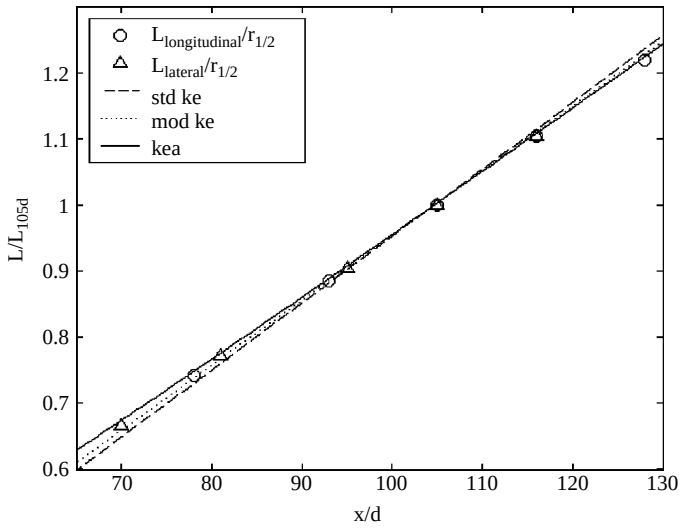

Figure 13.
Length scales on the symmetry plane

Table IV.
Measured and computed spreading rates in the axisymmetric jet flow

Meas.	$k\varepsilon$	$k\varepsilon\alpha$	Mod. $k\varepsilon$
0.1	0.1	0.1	0.1

$$U_1 \frac{\partial(k\alpha)}{\partial x_1} = k - \alpha\varepsilon \tag{45}$$

$$\gamma = \exp\left(-\frac{c_\alpha \alpha\varepsilon}{c_\tau k \sum_{i=0}^{n-1} \gamma^i}\right) \tag{46}$$

where U_1 is the mean velocity in the flow direction. This system of equations can be solved by means of a differential equation system solver, available for example in the commercial software Matlab 6.5, which was used in the present work to simulate the shear flow of Tavoularis and Corrsin (1981) and the first one (Case A) in Tavoularis and Karnik (1981).

The simulation results are shown in Figures 14-17.

The dissipation rate was estimated from the experimental data according to Tavoularis and Corrsin (1981). Figures 14-16 show that the predictions of the $k\varepsilon\alpha$ model are in better agreement with the experimental data than those of the $k\varepsilon$ model. In Figure 17, the $k\varepsilon$ model better predicts the development of the length scales than the $k\varepsilon\alpha$. The modified $k\varepsilon$ model gives significantly inferior results in all figures.

Regarding the boundary condition at the inlet, the $k\varepsilon\alpha$ model has the advantage of an additional variable, or "degree of freedom" which allows the specification of a correct Reynolds stress, as shown in Figure 16.

Discussion

In the benchmark flows that are examined, the $k\varepsilon\alpha$ model always provides a better or equivalent prediction of the mean flow field. Most notably the $k\varepsilon\alpha$ model predicts well

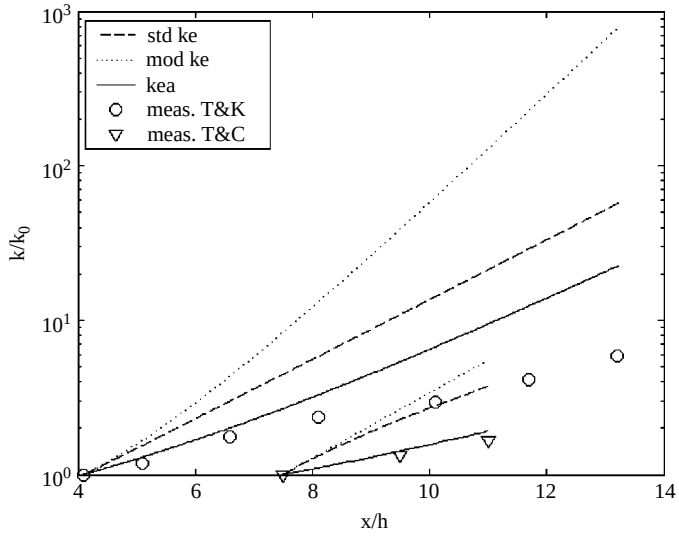

Notes: T&C stands for Tavoularis and Corrsin (1981), T&K for Tavoularis and Karnik (1981)

Figure 14.
Turbulent kinetic energy along the direction of the flow

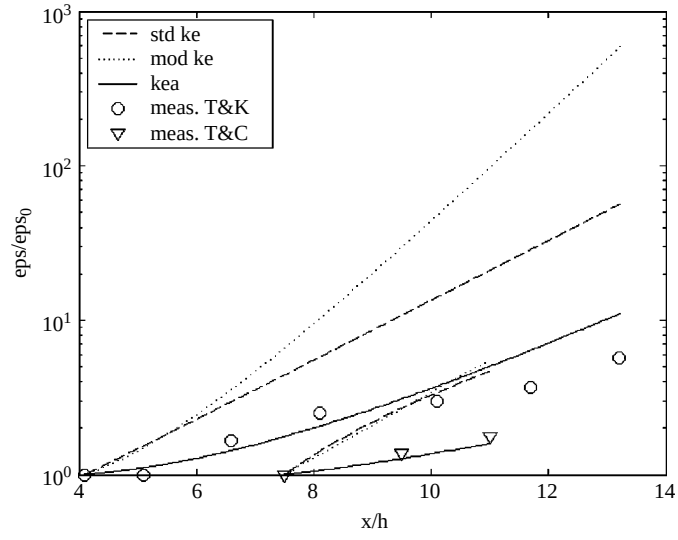

Note: Legend as in Figure 14

Figure 15.
Dissipation rate along the direction of the flow

the velocity profiles both in the axisymmetric and in the planar jet, significantly reducing the round-jet/plane-jet anomaly. Also the qualitative approach to self-similarity in the axisymmetric and plane jets described by Gutmark and Wygnanski (1976) is predicted by the $k\varepsilon\alpha$ model, while the opposite behaviour is computed with the standard $k\varepsilon$ model.

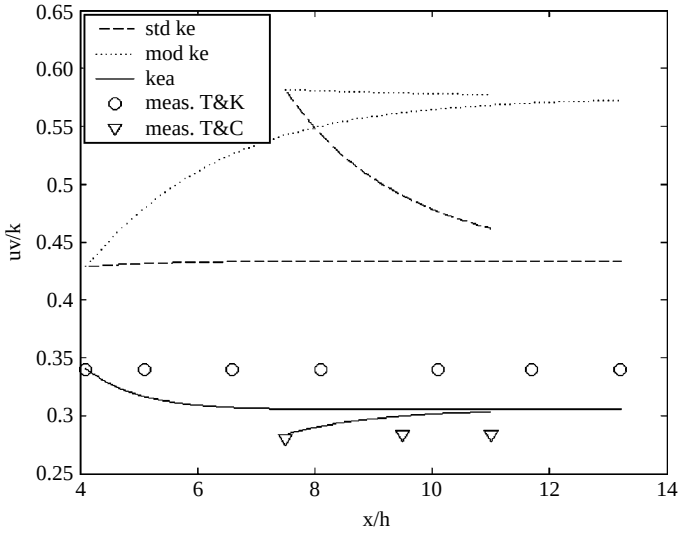

Figure 16.
Reynolds stress along the direction of the flow

Note: Legend as in Figure 14

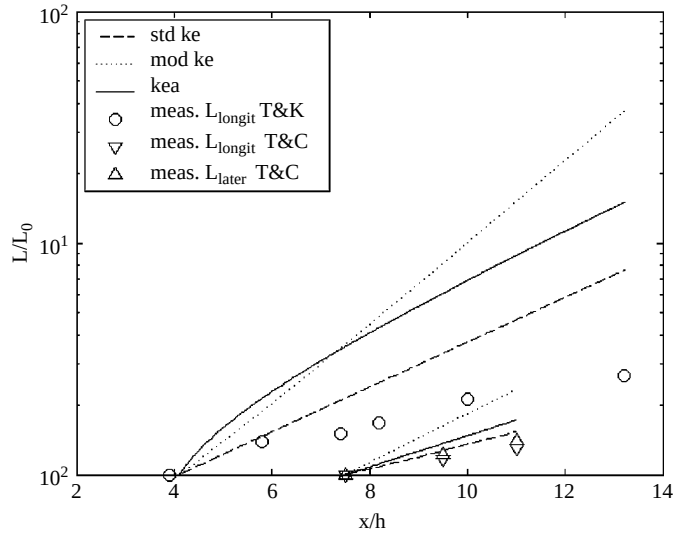

Figure 17.
Length scale along the direction of the flow

Note: Legend as in Figure 14

The computed turbulence intensities are also computed more accurately by the $k\varepsilon\alpha$ model than by the standard $k\varepsilon$ model, with the exception of the profile across the planar jet. An important difference regarding turbulence intensities is the value of the empirical constant c_2. This constant corresponds to the decay exponent (equation (37)) in grid turbulence, which has been studied extensively. Mohamed and LaRue (1990) show that most of the data can be reinterpreted to give little scatter around the value

$m = 1.3$. It is therefore difficult to justify the value $c_2 = 1.92$ ($m = 1.09$) used in the standard $k\varepsilon$ model, which lies outside of the experimental observed range (Pope, 2000). In other words it can be stated that the standard $k\varepsilon$ model does not represent correctly the fundamental power-law decay in grid turbulence, while the $k\varepsilon\alpha$ model does.

Also the modified version of the $k\varepsilon$ model, where the empirical constants have been substituted with the respective ones of the $k\varepsilon\alpha$ model, represents correctly the power law decay. In the modified $k\varepsilon$ furthermore, also the round-jet/plane-jet anomaly is significantly reduced. The performance of the modified $k\varepsilon$ model, however, is significantly inferior to those of the other models in the backward-facing step flow and in the homogeneous shear flows. These results show that the modification of the empirical constants can improve the performance of the $k\varepsilon$ model for certain flows, but it will inevitably worsen its performance for other flows, therefore not improving the generality of the model.

The length scales of turbulence are computed by the models only in the form of proportionality relations and therefore they are compared only in relative terms. The $k\varepsilon\alpha$ model better reproduces the relative scales in the axisymmetric jet case, while the standard $k\varepsilon$ model predicts a better trend in the shear flow case.

Regarding the characteristic time scales of turbulence τ_T, it should be noticed that the expression of τ_T in the $k\varepsilon\alpha$ model is not a proportionality relation as in the $k\varepsilon$ model, but it is an equality. This feature of the $k\varepsilon\alpha$ model is a substantial advantage, since it allows a direct comparison between the computed and the measured integral time scales (where available). A correct estimation of the time scales is especially important in reacting flows where the mixing time of the chemical species limits the progress of reaction.

A thorough study of the computational requirements was not performed because the focus of the work has been on the formulation and calibration of the model and on the accuracy of its results, so that the implementations have not been optimised numerically. It can be stated, however, that in the performed calculations the computational time required by the two models has been of the same order of magnitude.

Conclusions

It is argued that the age of turbulent energy α is a useful variable for characterising turbulence, and a method for computing α is proposed.

Two hypotheses are formulated. The first one is that the characteristic scales of turbulence are decreasing functions of α. The second one is that the effect of correlation on turbulent viscosity can be expressed as a function of α in analogy with the dispersion coefficient of a particle in a turbulent flow. Expressions for the turbulent viscosity and the characteristic scales are therefore proposed and they are integrated in a previous turbulence model. The resulting three-equations model gives generally better results than the original two-equations one. Most notably the $k\varepsilon\alpha$ model improves the prediction of the velocity profiles both in the axisymmetric and in the planar jet, eliminating the round-jet/plane-jet anomaly observed in the $k\varepsilon$ model. Furthermore, the model represents correctly the power-law decay behind grids gives a better estimation of the Reynolds stress in the homogeneous shear flow, both of which are miscalculated by the $k\varepsilon$ model.

These results support the hypotheses made and therefore are an encouragement to continue researching in this direction.

References

Adams, E.W. and Eaton, J.K. (1988), "An LDA study of the backward-facing step flow, including the effects of velocity bias", *Journal of Fluids Engineering*, Vol. 110, pp. 275-82.

Fluent Inc. (2003), *Fluent 6.1 Users Guide*, Fluent Inc., Lebanon, NH.

Ghirelli, F. and Leckner, B. (2004), "Transport equation for the local residence time of a fluid", *Chemical Engineering Science*, Vol. 59, pp. 513-23.

Gutmark, E. and Wygnanski, I. (1976), "The planar turbulent jet", *Journal of Fluid Mechanics*, Vol. 73, pp. 465-95.

Hanjalic, K., Launder, B.E. and Schiestel, R. (1980), "Multiple-time-scale concepts in turbulent shear flows", in Bradbury, L.J.S., Durst, F. and Launder, B.E. (Eds), *Turbulent Shear Flows 2*, Springer-Verlag, New York, NY, pp. 36-49.

Hussein, H.J., Capp, S.P. and George, W.K. (1994), "Velocity measurements in a high-Reynolds-number, momentum-conserving, axisymmetric, turbulent jet", *Journal of Fluid Mechanics*, Vol. 258, pp. 31-75.

Jones, W.P. (1994), "Turbulence modelling and numerical solution methods for variable density and combusting flows", in Libby, P.A. and Williams, F.A. (Eds), *Turbulent Reacting Flows*, Academic Press, London, pp. 355-8.

Kim, S.W. and Chen, C.P. (1989), "A multiple-time-scale turbulence model based on variable partitioning of the turbulent kinetic energy spectrum", *Numerical Heat Transfer*, Vol. 16, pp. 193-211.

Launder, B.E. and Spalding, D.B. (1974), "The numerical computation of turbulent flows", *Computer Methods in Applied Mechanics and Engineering*, Vol. 3, pp. 269-89.

Mohamed, M.S. and LaRue, J.C. (1990), "The decay power law in grid-generated turbulence", *Journal of Fluid Mechanics*, Vol. 219, pp. 195-214.

Pope, S.B. (2000), *Turbulent Flows*, Cambridge University Press, Cambridge.

Rubinstein, R. (2000), "Formulation of a two-scale model of turbulence", NASA/CR-2000-209853.

Tavoularis, S. and Corrsin, S. (1981), "Further experiments on the evolution of turbulent stresses and scales in uniformly sheared turbulence", *Journal of Fluid Mechanics*, Vol. 204, pp. 457-78.

Tavoularis, S. and Karnik, U. (1981), "Experiments in homogeneous sheared turbulence", *Journal of Fluid Mechanics*, Vol. 104, pp. 311-47.

Wygnanski, I. and Fielder, H. (1969), "Some measurements in the self-preserving jet", *Journal of Fluid Mechanics*, Vol. 38, pp. 577-612.

Appendix. Derivation of the α equation for a generic transported scalar

The derivation is presented here for a generic transported scalar z in a turbulent flow. The derivation is valid for scalars that diffuse due only to stochastic motion, i.e. where diffusion driven by enthalpy of mixing or other similar forces is negligible. The derivation is kept here as concise as possible. A more thorough one is presented in (Ghirelli and Leckner (2004)).

Given a spatial domain Ω the age α of the transported scalar z is defined as the time that z has spent inside Ω. For simplicity, it will be assumed in the following that Ω coincides with the computational domain. If z were a chemical species one could imagine to follow each molecule and to keep track of the time they spent inside Ω. If z were the turbulent energy, the concept is less intuitive, but nonetheless mathematically correct since k is represented as a scalar which is transported just as a chemical species.

The scalar θ is defined as follows:

$$\theta \equiv z\alpha. \tag{A1}$$

θ can be interpreted as an extensive variable corresponding to the intensive variable α. Since, z is transported by the flow, and α is a property of z, a transport equation can be written for θ. The equation represents the balance of θ over an infinitesimal control volume, as the classical transport equations in fluid mechanics. As such it includes an accumulation term, a convection one, a diffusion one, and a source term:

$$\frac{D\theta}{Dt} = \frac{\partial J_{\theta,i}}{\partial x_i} + s_\theta \tag{A2}$$

where $J_{\theta,i}$ is the diffusive flux of θ in direction x_i and s_θ is its source term. The left-hand side of the equation does not need much comment. The diffusion and source terms are less obvious. The source term will be considered first:

$$s_\theta = z - s_C\alpha \tag{A3}$$

where s_C is the sink term due to consumption of z (e.g. consumption of a species due to chemical reaction or consumption of k due to viscous dissipation). The first term on the right hand side of equation (A3) represents the source of θ due to the fact that the age of z grows with time. Since, α increases by one unit age per unit time, θ increases as $z^*1 = z$. This term is present only inside Ω. The second term on the right hand side of equation (A3) represents the sink of θ due to consumption of z. For example, when molecules of a species of age α disappear at a rate s_C due to a chemical reaction, θ disappears at a rate $s_\mathrm{C}\alpha$. Analogously, when turbulence of age α disappears at a rate ε, θ disappears at a rate $\varepsilon\alpha$. There is no source term corresponding to production of z in equation (A3) because at the moment z is produced, its residence time is zero. Production of z will therefore increase z but not θ resulting in a decrease of α.

The expression of the diffusive term in equation (A2) can be deduced by means of the hypothetical experiment described in the following. For this experiment, the scalar z is first defined as the sum of the concentrations of various species. It is later shown that also a more general definition of z can also be used:

$$z = \sum\nolimits_j X_j \tag{A4}$$

where j is an integer index and X_j is the concentration of species j. The experiment consists of injecting in a turbulent flow one pulse of each species at discrete times. α_j is the time that has elapsed since the pulse of species j was injected. α_j is clearly a function of time only.

Applying the Boussinesq hypothesis and making the assumption that molecular diffusion is negligible compared to turbulent diffusion, the diffusive flux of species j in direction x_1 can be written:

$$J_{j,1} = -D_\mathrm{T}\frac{\partial X_j}{\partial x_1} \tag{A5}$$

The diffusive flux of θ in direction x_1 can then be expressed as:

$$J_{\theta,1} = \sum\nolimits_j (J_{j,1}\alpha_j) = -\sum\nolimits_j (D_\mathrm{T}\frac{\partial X_j}{\partial x_1}\,\alpha_j) = -D_\mathrm{T}\frac{\partial}{\partial x_1}(\sum\nolimits_j X_j\alpha_j) \tag{A6}$$

Because α_j is not a function of x_1. Furthermore:

$$J_{\theta,1} = -D_T \frac{\partial}{\partial x_1}\left(\sum_j X_j \alpha_j\right) = -D_T \frac{\partial}{\partial x_1}\left(\sum_j X_j \frac{\sum_j X_j \alpha_j}{\sum_j X_j}\right) = -D_T \frac{\partial}{\partial x_1}(z\bar{\alpha}) = -D_T \frac{\partial \theta}{\partial x_1} \quad \text{(A7)}$$

where the overbar denotes an average. (In equation (A1) the average is not explicitly stated, but it is understood, because α is regarded as a continuous property. As such, it is the average age of the molecules inside the control volume.)

In the above discussion, several species X_j have been used to provide a clear picture of the hypothetical experiment. By using a different species at every pulse, the various fractions of z have been "marked" so that they can be followed. The transport of the various species, however, takes place independently of the nature of the species, since it was assumed that molecular diffusion is negligible. In other words, if the same species had been used at every pulse, the result would be the same, even if in practice one would not be able to keep track of which molecules were injected at a certain time. Similarly, the reasoning can be applied to any transported scalar z that can be divided in arbitrary fractions that diffuse according to the same expression as the whole z. (This would not be the possible, for example, if the various species in the hypothetical experiment were characterized by different diffusivities D_j, in which case equations (A6) and (A7) could not be written. Also in the case that z represented a species that diffuses mainly due to enthalpy of mixing, it would not be correct to divide z in arbitrary fractions and assume that they should diffuse according to the same law as the whole z. This is explained in more detail by Ghirelli and Leckner (2004).)

Regarding diffusion of turbulent kinetic energy k, it is reasonable to assume that all fractions of k (for example, energy at all the frequencies) are transported according to the same expression, analogous to equation (A5).

In conclusion, the hypothetical experiment shows that the diffusive flux of θ can be expressed according to equation (A7). Therefore, the equation of transport of the age of z can be written as:

$$\frac{D(z\alpha)}{Dt} = \frac{\partial}{\partial x_i}\left(D_z \frac{\partial(z\alpha)}{\partial x_i}\right) + z - \alpha s_C \quad \text{(A8)}$$

where D_z is the diffusivity of z. In the $k\varepsilon\alpha$ model presented above, the diffusivity of k is taken to be the sum of the molecular and turbulent viscosities.

About the author

Federico Ghirelli has a PhD degree in energy conversion engineering. He studies modelling of various combustion systems, e.g. grate furnaces, fluidised bed combustors and swirling burners. His main interests are modelling of gas-phase reaction rates, fluid residence time and turbulence. Federico Ghirelli can be contacted at: federico.ghirelli@alice.it